

Synthesis and Characterization of Amorphous Silica Nanoparticles Production from Indonesia Coal Fly Ash

Yugo Chambioso¹, Ariadne Lakshmidevi Juwono^{1*}, Amru Daulay²

¹Department of Physics, Faculty of Mathematics and Natural Sciences, Universitas Indonesia, Depok, 16424, Indonesia

²Research Center for Mineral Technology, National Research and Innovation Agency (BRIN), Jl. Ir. Sutami, Km. 15, Tanjung Bintang, South Lampung, Lampung, Indonesia

*Corresponding Author: ariadne.laksmidevi@ui.ac.id

ARTICLE INFO

Article history:

Received 04 November 2025

Revised 24 November 2025

Accepted 25 November 2025

Available online 04 December 2025

E-ISSN: [2656-1492](https://doi.org/10.32734/jcnar.v7i2.23383)

How to cite:

Yugo Chambioso, Ariadne Lakshmidevi Juwono, Amru Daulay. Synthesis and Characterization of Amorphous Silica Nanoparticles Production from Indonesia Coal Fly Ash. Journal of Chemical Natural Resources. 2025, 7(2):96-104.

ABSTRACT

Coal fly ash an inexpensive waste material rich in silica, is reused as a renewable source and has attracted widespread attention. The sol-gel process was used to synthesize silica nanoparticles based on coal fly ash. Extraction of silica in the form of alkaline sodium silicate using alkali, followed by the formation of silica gel from the neutralization of alkaline sodium silicate with acid. The treated samples were calcined at 450 °C, 650 °C, and 850 °C. The chemical composition, morphology, phase, and silica functional groups of the as-synthesized silica nanoparticle powder were investigated using X-ray fluorescence (XRF), field emission scanning electron microscopy and Electron diffraction spectroscopy (FESEM-EDS), Fourier transform infrared spectroscopy (FTIR), and X-ray diffraction (XRD). Infrared (IR) spectral analysis showed that silica had hydrogen-bonded silanol and siloxane groups. The silica nanoparticles' purity was found to be as high as 97% in their amorphous state, with XRD analysis indicating this due to the broad peak observed in the 20-23° two-theta region, characterised by a spherical shape and a tendency to aggregate into clusters.

Keyword: Nanomaterial, Waste, Coal fly ash, Silica nanoparticles, Sol-gel.

ABSTRAK

Abu terbang batu bara, bahan limbah yang murah dan kaya akan silika, digunakan kembali sebagai sumber daya terbarukan dan telah menarik perhatian luas. Metode sol-gel digunakan untuk mensintesis nanopartikel silika berbasis abu terbang batu bara. Ekstraksi silika dalam bentuk natrium silikat alkali menggunakan alkali, diikuti dengan pembentukan gel silika dari netralisasi natrium silikat alkali dengan asam. Sampel yang telah melalui proses sol-gel dikalsinasi pada suhu 450 °C, 650 °C, dan 850 °C. Komposisi kimia, morfologi, fasa, dan kelompok fungsional silika pada bubuk nanopartikel silika yang disintesis dianalisis menggunakan *X-ray fluorescence* (XRF), *Field Emission Scanning Electron Microscopy and Electron Diffraction Spectroscopy* (FESEM-EDS), *Fourier Transform Infrared Spectroscopy* (FTIR), and *X-ray Diffraction* (XRD). Analisis FTIR menunjukkan adanya kelompok silanol dan siloksan yang terikat hidrogen dalam silika. Kemurnian nanopartikel silika mencapai 97% dalam bentuk amorf, seperti yang dikonfirmasi oleh XRD puncak lebar dari daerah $2\theta = 20-23^\circ$, yang memiliki bentuk partikel bulat dan kecenderungan untuk membentuk kluster.

Kata kunci: Nanomaterial, Limbah, Abu terbang batu bara, Nanopartikel silika, Sol-gel.

1. Introduction

The majority of minerals on the Earth's surface are comprised of silica, a substance that ranks as the second most abundant element found on the planet's surface [1]. Silicon dioxide, more commonly referred to as silica (SiO₂), possesses numerous notable properties that make it suitable for a range of applications. These properties include strength, mechanical properties, controllable pore size, and relatively harmless chemical makeup [2]. Currently, nanomaterials comprised of silica are making a substantial contribution to technological progress across a range of applications due to their minute size and extensive surface area [3]. Currently, nanomaterials comprised of silica are making a substantial contribution to technological progress across a range of



This work is licensed under a Creative Commons Attribution-ShareAlike 4.0 International.
<https://doi.org/10.32734/jcnar.v7i2.23383>

applications due to their minute size and extensive surface area [3]. Silica nanoparticles are used as catalysts [3] water purification [4] rubber [5] solar cells [6] agriculture [7] biomaterials [8] and construction materials [9]. Mostly, physical methods like top-down approaches are used to get silica nanoparticles [10] and bottom-up approaches (e.g., chemical) techniques [7]. Silica nanoparticles can be generated from industrial wastes such as fly ash [11] quartz sand [7] rice husk ash [12] palm kernel shell [13] and sugarcane ash [14] which can be reused to achieve a sustainable cycle and long-term strategy of the industry. In Indonesia, approximately 60% of power is generated by the coal powerplant industry. The by-product is fly ash in the form of solids, which is usually piled up at the industrial site which can pollute the environment and damage land [15]. Unused fly ash must be used to protect the environment. This can be accomplished by reutilizing fly ash as a silica source in the synthesis of silica nanoparticles. Several methods exist for synthesizing silica nanoparticles from coal fly ash, such as the precipitation process [16], sodium silicate solution with the aid of a surfactant [17], microwave irradiation [18], and hydrothermal methods [19]. The sol-gel process stands out among other methods due to its versatility and high efficiency, enabling high purity, mild reactions, and homogeneous results [20].

The present study differs from many previous reports by using coal fly ash, creating a more challenging and industrially realistic feedstock. To address this impurity burden, the solvent concentration and precipitation parameters were specifically optimized to maximize silica recovery. Scientists created an uncomplicated and affordable way to produce high-purity amorphous silica nanoparticles from Indonesian coal fly ash. Using the techniques of alkali extraction, acid precipitation, and controlled calcination. Despite extensive research on nanosilica, most reported methods remain confined to laboratory-scale conditions and rely on high-purity precursors, limiting their suitability for industrial production. Scalable, waste-based extraction routes have received little attention, particularly those capable of handling impurity-rich coal fly ash. This study aims to fill this gap by refining a straightforward and flexible nanosilica extraction process. This study utilizes a major industrial byproduct, and also showcases the potential of fly ash as a sustainable and renewable source for the production of nanomaterials.

2. Research and Methodology

2.1. Materials

Coal fly ash was collected from the Tarahan thermal power plants located in Lampung, Indonesia. The chemical reagents including Sodium hydroxide (NaOH; 98 wt%) and Hydrochloric Acid (HCl; 37 wt%) were acquired from Merck in Germany, and used without additional purification.

2.2. Synthesis of silica nanoparticles

A mixture of 60 g fly ash and 0.6 mol NaOH). The mixture was stirred at 600 rpm at 180 °C for 1 h. The solution was cooled to room temperature, and after that, it was filtered and yielded a light-yellow filtrate. The solution was added dropwise at a rate of approximately 1 mL/min with 0.5 mol HCl until it reached pH 4 (suitable balance between the hydrolysis and condensation of silica nanoparticles) and a white solid formed as a precipitate. The precipitate was thoroughly rinsed with distilled water multiple times until its pH reading stabilised at 7. The sample was then heated to 120 °C for a period of 6 hours and subsequently underwent calcination in a muffle furnace for 3 hours at temperatures of 450 °C, 650 °C, and 850 °C.

2.3. Characterization Technique

Silica samples were characterized by X-Ray Diffraction (XRD, PanAnalytical type X'PertPro) using Cu K α radiation at wavelength of 1.54 Å to investigate their structure. The morphological and chemical compositions were characterised using field emission scanning electron microscopy–energy dispersive spectroscopy (FESEM-EDS Quattro S). Bruker INVENIO type Fourier transform infrared spectroscopy was employed to verify the silica functional group, with FTIR measurements taken between 400–4000 cm⁻¹. The silica content and amount of metallic impurities in the sample were determined using X-Ray Fluorescence (a PanAnalytical Minipal 4 XRF). Nitrogen physisorption was performed using N₂ adsorption with the Quantachrome TouchWin v1.11 software, capturing the adsorption and desorption of N₂ at 77 K after a 1-hour degassing period at 565 K.

3. Results and Discussion

3.1. X-Ray Fluorescence (XRF)

Characterization using XRF was carried out to determine the chemical composition of the coal fly ash and silica nanoparticles (SiO₂), as presented in Table 1.

Table 1. XRF analysis of coal fly ash and silica nanoparticles.

Coal fly ash		Silica nanoparticles			
Elements	Conc. (%)	Elements	Conc. (%)		
			450 °C	650 °C	850 °C
SiO ₂	50.20	SiO ₂	97.41	97.61	97.57
Al ₂ O ₃	5.23	Al ₂ O ₃	0.28	1.37	1.27
P ₂ O ₅	0.49	P ₂ O ₅	0.73	0.58	0.62
CaO	0.50	CaO	0.28	0.31	0.24
Fe ₂ O ₃	31.33	Fe ₂ O ₃	0.12	-	0.10
TiO ₂	0.53	TiO ₂	0.17	-	0.15
SO ₃	8.74	SO ₃	-	-	-
K ₂ O	1.46	K ₂ O	-	-	-
As ₂ O ₃	0.36	As ₂ O ₃	-	-	-

The chemical composition of the coal fly ash samples, as determined by XRF analysis, is presented in table 1. It mainly contains SiO₂ (50.20%), Al₂O₃ (5.23%), and Fe₂O₃ (31.33%). XRF analysis confirmed that the coal fly ash contained 50.20 wt% of SiO₂. Nevertheless, the silica yield declined as the calcination temperature increased, with values of 16.60% at 450 °C, 13.28% at 650 °C, and 7.75% at 850 °C, based on the theoretical SiO₂ content. The observed reduction in yield at higher temperatures may be attributed to enhanced sintering or phase transformations, which potentially limit the effectiveness of silica extraction. After the synthesis process, a number of chemical compounds detected in coal fly ash were initially no longer identified in the resulting silica nanoparticles. This is attributed to the various stages of the chemical process, including dissolution, precipitation, and purification, which effectively remove the compounds. In addition, redistribution in the silica nanoparticle matrix plays an important role, as the compounds accumulate in the residual solids separated from the sodium silicate solution. Silica with a purity of up to 97%, and similar findings using the sol-gel method obtained a purity of 94% [21]. The purity of the extracted silica was analyzed via XRF. The SiO₂ purity value was obtained directly from the oxide composition profile generated by XRF, in which SiO₂ accounted for 97% of the total oxide mass. Therefore, the reported purity corresponds to the relative abundance of SiO₂ with respect to all detected oxides. In addition, the alkali fusion method using the acid precipitants H₂SO₄ and CH₃COOH obtained silica nanoparticles purities of 95.33% and 69.25%, respectively [22,23]. The difference in purity is likely influenced by the method used, the solution concentration, and the calcination temperature. Following the sol-gel process, the silica material had a purity level of 97%, signifying that the method was effective.

Table 2. Silica nanoparticles synthesis using sol-gel methods reported in previous studies.

Reference	Raw Material	Acid	Key Conditions	Purity (%)
[24]	Mission grass	2M HCl	settle for 12 h and filtered	95.61%
[25]	Rice husk ash	1N HCl	pH 6	95%
[11]	Fly ash	1-2M HCl	pH10	94%
[13]	Palm kernel shell ash	2N HCl	pH 7.5-8.5	96,83%
[26]	Burnt paddy husk	1N HCl	pH 7	90.44%
[27]	Palm ash	2% Citric acid	70 °C of solution temperature	92%
[28]	Rice straw	10% H ₂ SO ₄	-	96%

3.2. Fourier Transform Infrared (FTIR)

The region exhibited three characteristic bands of silica between 400-1200 cm⁻¹. Peaks at 1048 cm⁻¹, 796 cm⁻¹, and 446 cm⁻¹ are characteristic of silica [29]. Peaks typically occur between 793 and 1050 cm⁻¹ when samples include Si-O bonds [7]. The broad band at 1048 cm⁻¹ was attributed to the stretching vibration of Si-O [30]. The peak at 796 cm⁻¹ arises from symmetric Si-O-Si stretching mode vibrations [31] and the peak at 446 cm⁻¹ is due to Si-O-Si bending vibrations. The broad absorption band observed around 1633 cm⁻¹ is attributed to the stretching vibration of H₂O molecules, likely originating from moisture retained within the porous structure of the aerogels [32]. Additionally, the presence of distinct -OH stretching vibrations indicates that water molecules were adsorbed from the environment post-calcination. This behavior reflects the hygroscopic nature of silica particles, as they readily attract and retain moisture from ambient air [33]. The FTIR spectroscopy results indicate that all samples at different temperatures contained Si and O.

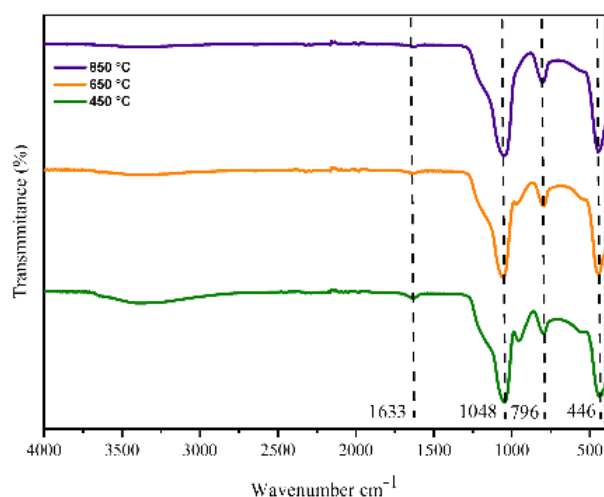


Figure 1. FTIR spectra of silica nanoparticles calcined at various temperatures.

3.3. X-Ray Diffraction (XRD)

Figure 2. Diffractograms of silica nanoparticles forms at different calcination temperatures. The absorption patterns of the three samples were identical, supporting the presence of pure, amorphous silica and indicating no sharp intensity peaks [34]. However, weak intensity peaks obtained from other minerals as listed in table 1. The peak intensity and diffraction width were around $2\theta = 21-23^\circ$ [35], silica nanoparticles are primarily amorphous and relatively small in size, as verified by Zulkifli et al., [36]. The amorphous nature was confirmed by the lack of sharp peaks, which suggests the absence of an organized form of silica [37].

Minor XRD peaks detected at $2\theta = 43-44^\circ$ confirm the presence of corundum (Al_2O_3), which is known as a highly stable crystalline phase resistant to decomposition even under strong alkaline conditions [38]. The persistence of this phase indicates that a fraction of alumina remains inert and structurally intact, contributing to the crystalline backbone of the system. At elevated temperatures (850 °C), the amorphous hump diminishes while sharper diffraction peaks become evident, suggesting partial recrystallization as a consequence of thermal sintering [39]. This structural evolution reflects the conversion of amorphous aluminosilicate phases into more ordered crystalline domains, which can alter the reactivity and densification behavior of the material. Such recrystallization not only reduces the availability of reactive sites for further pozzolanic activity but may also enhance thermal stability and mechanical rigidity, depending on the balance between crystalline and amorphous phases [40].

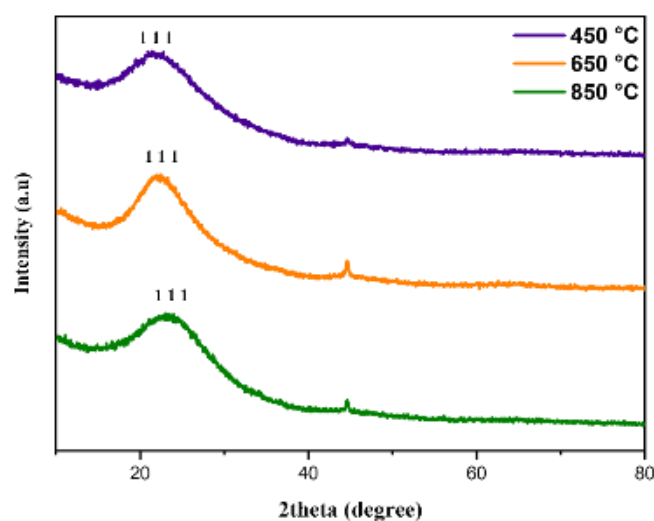


Figure 2. X-Ray diffraction patterns of silica nanoparticles calcined at various temperatures.

3.4. Pore Structure Analysis

Figure 3 illustrates characteristic nitrogen adsorption-desorption isotherms and BJH pore size distributions for silica nanoparticles that have been heat-treated at multiple temperatures. The isotherms for nitrogen

adsorption-desorption of samples heated to 450 °C, 650 °C, and 850 °C are shown in Figure 3a-c. All isotherms exhibit a progressive increase in adsorption capacity with increasing relative pressure (P/P_0), with a sharp uptake observed as P/P_0 approaches 1. This behavior indicates the occurrence of capillary condensation, which is characteristic of mesoporous materials. The IUPAC classification indicates that the obtained curves are type IV isotherms, which are usually found in mesoporous solids [41]. The existence of a hysteresis loop in the medium to high-pressure region indicates the presence of slit-like or ink-bottle pore structures, which is consistent with the characteristics of silica-based materials.

The pore size distribution shown in the figure is presented in Figure 3a–c on the right. The sample calcined at 450 °C exhibits a relatively broad distribution, with a dominant pore size ranging between 40–120 nm, indicating the prevalence of larger mesopores. At 650 °C, the distribution becomes narrower, with pores primarily centered in the range of 10–20 nm, signifying the formation of intermediate mesopores. The sample treated at 850 °C has its pore size distribution more finely defined, primarily focused within a 5–20 nm range, with the principal peak occurring at approximately 15 nm. These changes suggest that higher calcination temperatures play a crucial role in reducing and stabilizing pore sizes, while maintaining mesoporosity [42].

Overall, the analysis confirms that the synthesized silica materials belong to the category of mesoporous silica, with a clear shift toward smaller and more uniform pore sizes at elevated calcination temperatures. The phenomenon in question is due to the structural rearrangement of the silica framework, which occurs during thermal treatment, resulting in larger pores partially collapsing or shrinking and the formation of more uniform mesopores. Such characteristics are highly desirable, as a high specific surface area combined with narrow pore size distribution directly enhances adsorption activity and improves the reactivity of the material in applications such as cementitious composites and catalysis.

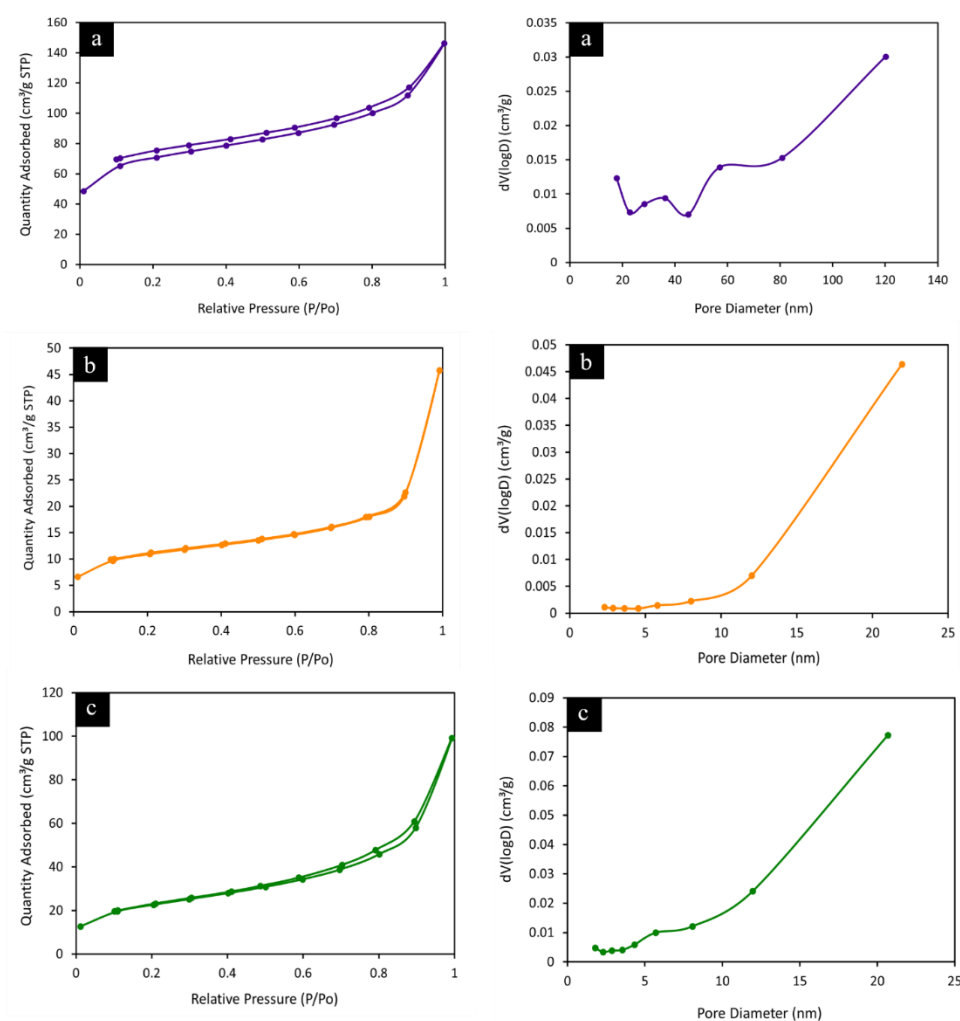


Figure 3. The adsorption/desorption isotherms for N₂ and BJH pore size distribution of silica nanoparticles were measured following calcination at three specific temperatures: 450 °C, 650 °C, and 850 °C.

3.5. Field-Emission Scanning Electron Microscopy (FESEM) and Energy Dispersive Spectroscopy (EDS)

FESEM images and chemical analyses of the silica nanoparticles calcined at various temperatures are presented in Figure 4. Images of spherical structures in Figure 4 were obtained using FESEM. The morphology of the particles is clearly evident, in agreement with Arunmetha et al. research findings [43], who observed similar spherical forms and homogeneous. FESEM images revealed that the particles mainly had a spherical shape and relatively consistent sizes. Primary observations of particle clustering and agglomeration resulted from the strong intermolecular forces between silica nanoparticles [24]. Following the sol-gel process, the silica material had a purity level of 97%, signifying that the method was effective. Due to their high surface energy, nanoparticles typically aggregate into clusters naturally. The high surface energy of nanoparticles prompts agglomeration as a way to decrease surface energy by minimising the exposed area. However, when particles cluster together, their effective contact area decreases. Consequently, during sintering, this condition leads to the formation or collapse of pores, ultimately resulting in a decrease in the total surface area [44]. Yadav et al. [21], their study also reported that cluster formation and aggregation by spherical nano-sized silica from fly ash are shown in Figure 4.

Analysis of silica nanoparticles using EDS after calcination at 450 °C, 650 °C, and 850 °C showed peaks corresponding to silicon, oxygen, and carbon. Confirmation of the primary atomic composition was achieved, with Si and O present as expected, and the silica nanoparticles were found to have a purity of approximately 94-97% [21]. The EDS data obtained at 850 °C shows that the dominant peak is carbon (C) due to the sample preparation treatment before characterization, which resulted in adhesive tape and also comes from the raw material, fly ash carbon.

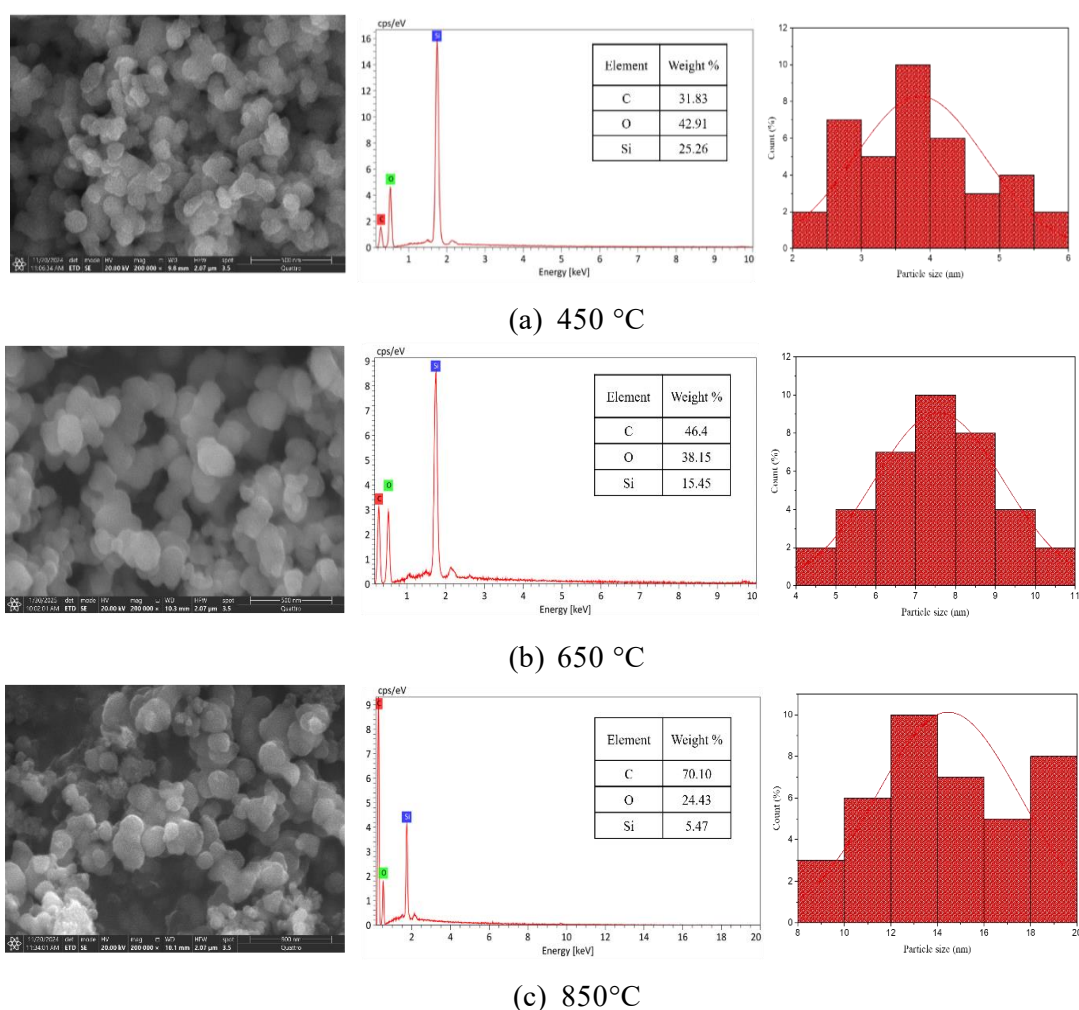


Figure 4. Morphological analysis was conducted on silica nanoparticles that were heated at various temperatures: (a) 450 °C, (b) 650 °C, and (c) 850 °C, as indicated by a scale bar of 500 nm.

4. Conclusion

In summary, silica nanoparticles were synthesised from coal fly ash through a sol-gel process, resulting in high yields that are suitable for silica nanoparticles. According to XRD analysis, the silica nanoparticles in an amorphous form had a purity of up to 97%, as evidenced by the broad hump in the 20-23° two-theta region, which exhibited a spherical shape and a propensity to form clusters. Analysis of the infrared (IR) spectrum showed that silica contains hydrogen-bonded silanol and siloxane groups. Based on the obtained purity results, the product can be used for electronics, medicine, agriculture and in construction and building materials. The successful synthesis of pure silica nanoparticle powders was possible using the method described in this study.

5. Acknowledgment

The authors would like to express their gratitude to the research supported by the Lembaga Pengelola Dana Pendidikan (LPDP) scholarship with identification number 202311112857302 and sponsored by the National Research and Innovation Agency (BRIN).

6. Conflicts of Interest

The authors state that there are no conflicts of interest relating to the publication of this paper.

References

- [1] B.S. Tubaña, J.R. Heckman, Silicon in soils and plants, in: *Silicon and Plant Diseases*, Springer International Publishing, 2015: pp. 7–51. https://doi.org/10.1007/978-3-319-22930-0_2.
- [2] L. Chen, J. Liu, Y. Zhang, G. Zhang, Y. Kang, A. Chen, X. Feng, L. Shao, The toxicity of silica nanoparticles to the immune system, *Nanomedicine* 13 (2018) 1939–1962. <https://doi.org/10.2217/nmm-2018-0076>.
- [3] A. Ramazani, Review on the synthesis and functionalization of SiO₂ nanoparticles as solid supported catalysts, *Curr Org Chem* 21 (2017) 908–922.
- [4] P.G. Jeelani, P. Mulay, R. Venkat, C. Ramalingam, Multifaceted Application of Silica Nanoparticles. A Review, *Silicon* 12 (2020) 1337–1354. <https://doi.org/10.1007/s12633-019-00229-y>.
- [5] J.W. van Hoek, G. Heideman, J.W.M. Noordermeer, W.K. Dierkes, A. Blume, Implications of the use of silica as active filler in passenger car tire compounds on their recycling options, *Materials* 12 (2019). <https://doi.org/10.3390/ma12050725>.
- [6] J. Singh, *Excitonic and Photonic Processes in Materials*, 2015.
- [7] C. Van Hoang, D.N. Thoai, N.T.D. Cam, T.T.T. Phuong, N.T. Lieu, T.T.T. Hien, D.N. Nhiem, T.D. Pham, M.H.T. Tung, N.T.T. Tran, A. Mechler, Q. V. Vo, Large-Scale Synthesis of Nanosilica from Silica Sand for Plant Stimulant Applications, *ACS Omega* 7 (2022) 41687–41695. <https://doi.org/10.1021/acsomega.2c05760>.
- [8] W. Tan, K. Wang, X. He, X.J. Zhao, T. Drake, L. Wang, R.P. Bagwe, Bionanotechnology based on silica nanoparticles, *Med Res Rev* 24 (2004) 621–638. <https://doi.org/10.1002/med.20003>.
- [9] K. Khan, M.A.M. Johari, M.N. Amin, M. Iqbal, Evaluation of the mechanical properties, microstructure, and environmental impact of mortar incorporating metakaolin, micro and nano-silica, *Case Studies in Construction Materials* 20 (2024). <https://doi.org/10.1016/j.cscm.2023.e02699>.
- [10] A. Agrawal, G.C. Yi, Sample pretreatment with graphene materials, in: *Comprehensive Analytical Chemistry*, Elsevier B.V., 2020: pp. 21–47. <https://doi.org/10.1016/bs.coac.2020.08.012>.
- [11] V.K. Yadav, M.H. Fulekar, Green synthesis and characterization of amorphous silica nanoparticles from fly ash, 2019. www.sciencedirect.com/www.materialstoday.com/proceedings2214-7853.
- [12] S. Saini, A. Gupta, A.J. Mehta, S. Pramanik, Rice husk-extracted silica reinforced graphite/aluminium matrix hybrid composite, *J Therm Anal Calorim* 147 (2022) 1157–1166. <https://doi.org/10.1007/s10973-020-10404-8>.
- [13] F. Farirai, M. Mupa, M.O. Daramola, An improved method for the production of high purity silica from sugarcane bagasse ash obtained from a bioethanol plant boiler, *Particulate Science and Technology* 39 (2021) 252–259. <https://doi.org/10.1080/02726351.2020.1734700>.
- [14] P.E. Imoisili, K.O. Ukoba, T.C. Jen, Synthesis and characterization of amorphous mesoporous silica from palm kernel shell ash, *Boletín de La Sociedad Española de Cerámica y Vidrio* 59 (2020) 159–164. <https://doi.org/10.1016/j.bsecv.2019.09.006>.
- [15] P. Duan, C. Yan, W. Zhou, D. Ren, Development of fly ash and iron ore tailing based porous geopolymer for removal of Cu(II) from wastewater, *Ceram Int* 42 (2016) 13507–13518. <https://doi.org/10.1016/j.ceramint.2016.05.143>.

- [16] S.M.T. Al-Abboodi, E.J.A. Al-Shaibani, E.A. Alrubai, Preparation and Characterization of Nano silica Prepared by Different Precipitation Methods, in: IOP Conf Ser Mater Sci Eng, IOP Publishing Ltd, 2020. <https://doi.org/10.1088/1757-899X/978/1/012031>.
- [17] M.E. Aphane, E.D. Maggott, F.J. Doucet, S.F. Mapolie, M. Landman, E.M. van der Merwe, Synthesis and Evaluation of Mesoporous Silica Nanoparticle Catalyst Supports Prepared from South African Coal Fly Ash, *Waste Biomass Valorization* 15 (2024) 5053–5068. <https://doi.org/10.1007/s12649-024-02496-2>.
- [18] A.S. Matlob, R.A. Kamarudin, Z. Jubri, Z. Ramli, Using the Response Surface Methodology to Optimize the Extraction of Silica and Alumina from Coal Fly Ash for the Synthesis of Zeolite Na-A, *Arab J Sci Eng* 37 (2012) 27–40. <https://doi.org/10.1007/s13369-011-0149-2>.
- [19] P.E. Imoisili, K.O. Ukoba, T.C. Jen, Synthesis and characterization of amorphous mesoporous silica from palm kernel shell ash, *Boletin de La Sociedad Espanola de Ceramica y Vidrio* 59 (2020) 159–164. <https://doi.org/10.1016/j.bsecv.2019.09.006>.
- [20] T. Dippong, E.A. Levei, O. Cadar, A. Mesaros, G. Borodi, Sol-gel synthesis of CoFe₂O₄:SiO₂ nanocomposites – insights into the thermal decomposition process of precursors, *J Anal Appl Pyrolysis* 125 (2017) 169–177. <https://doi.org/10.1016/j.jaap.2017.04.005>.
- [21] V.K. Yadav, M.H. Fulekar, Green synthesis and characterization of amorphous silica nanoparticles from fly ash, 2019. www.sciencedirect.com/www.materialstoday.com/proceedings2214-7853.
- [22] C. Zhou, Q. Gao, W. Luo, Q. Zhou, H. Wang, C. Yan, P. Duan, Preparation, characterization and adsorption evaluation of spherical mesoporous Al-MCM-41 from coal fly ash, *J Taiwan Inst Chem Eng* 52 (2015) 147–157. <https://doi.org/10.1016/j.jtice.2015.02.014>.
- [23] D. Li, H. Min, X. Jiang, X. Ran, L. Zou, J. Fan, One-pot synthesis of Aluminum-containing ordered mesoporous silica MCM-41 using coal fly ash for phosphate adsorption, *J Colloid Interface Sci* 404 (2013) 42–48. <https://doi.org/10.1016/j.jcis.2013.04.018>.
- [24] A. Thayyullathil, C.M. Naseera, F.M. Liyakhath, E.K. Vydhehi, S.R. Sheeja, S. Naduparambath, S. Sasidharan, Effect of Temperature and Method of Synthesis on Morphology and Phase Transition of Amorphous and Crystalline Nano Silica Extracted from Mission Grass (*Pennisetum Polystachion*), *Silicon* 16 (2024) 3491–3501. <https://doi.org/10.1007/s12633-024-02932-x>.
- [25] J. Nayak, J. Bera, A Simple Method for Production of Humidity Indicating Silica Gel from Rice Husk Ash, 2009.
- [26] K. V Selvakumar, A. Umesh, P. Ezhilkumar, S. Gayatri, P. Vinith, V. Vignesh, Extraction of Silica from Burnt Paddy Husk, 2014.
- [27] C.P. Faizul, C. Abdullah, B. Fazlul, Extraction of Silica from Palm Ash via Citric Acid Leaching Treatment, 2013.
- [28] M.S.U. Rehman, M.A. Umer, N. Rashid, I. Kim, J.I. Han, Sono-assisted sulfuric acid process for economical recovery of fermentable sugars and mesoporous pure silica from rice straw, *Ind Crops Prod* 49 (2013) 705–711. <https://doi.org/10.1016/j.indcrop.2013.06.034>.
- [29] N. Thuadaij, A. Nuntiya, Synthesis and Characterization of Nanosilica from Rice Husk Ash Prepared by Precipitation Method, 2008.
- [30] M. Mehravar, B.B.F. Mirjalili, E. Babaei, A. Bamoniri, Nano-SiO₂/DBN: an efficacious and reusable catalyst for one-pot synthesis of tetrahydrobenzo[b]pyran derivatives, *BMC Chem* 15 (2021). <https://doi.org/10.1186/s13065-021-00760-3>.
- [31] R. Yuvakkumar, V. Elango, V. Rajendran, N. Kannan, High-purity nano silica powder from rice husk using a simple chemical method, *J Exp Nanosci* 9 (2014) 272–281. <https://doi.org/10.1080/17458080.2012.656709>.
- [32] M. Shahjahan, Synthesis and Characterization of Silver Nanoparticles by Sol-Gel Technique, *Nanoscience and Nanometrology* 3 (2017) 34. <https://doi.org/10.11648/j.nsnm.20170301.16>.
- [33] O.A. Hodhod, M.S. Khalafalla, M.S.M. Osman, ANN models for nano silica/ silica fume concrete strength prediction, *Water Science* 33 (2019) 118–127. <https://doi.org/10.1080/11104929.2019.1669005>.
- [34] A.A. Alshatwi, J. Athinarayanan, V.S. Periasamy, Biocompatibility assessment of rice husk-derived biogenic silica nanoparticles for biomedical applications, *Materials Science and Engineering C* 47 (2015) 8–16. <https://doi.org/10.1016/j.msec.2014.11.005>.
- [35] C. li Liu, S. li Zheng, S. hua Ma, Y. Luo, J. Ding, X. hui Wang, Y. Zhang, A novel process to enrich alumina and prepare silica nanoparticles from high-alumina fly ash, *Fuel Processing Technology* 173 (2018) 40–47. <https://doi.org/10.1016/j.fuproc.2018.01.007>.

- [36] N.S.C. Zulkifli, I. Ab Rahman, D. Mohamad, A. Husein, A green sol-gel route for the synthesis of structurally controlled silica particles from rice husk for dental composite filler, *Ceram Int* 39 (2013) 4559–4567. <https://doi.org/10.1016/j.ceramint.2012.11.052>.
- [37] J. Shim, P. Velmurugan, B.T. Oh, Extraction and physical characterization of amorphous silica made from corn cob ash at variable pH conditions via sol gel processing, *Journal of Industrial and Engineering Chemistry* 30 (2015) 249–253. <https://doi.org/10.1016/j.jiec.2015.05.029>.
- [38] C. li LIU, S. hua MA, J. DING, Y. LUO, S. li ZHENG, Y. ZHANG, Kinetics of decomposition of mullite and corundum in coal fly ash under highly alkaline condition, *Transactions of Nonferrous Metals Society of China (English Edition)* 29 (2019) 868–875. [https://doi.org/10.1016/S1003-6326\(19\)64997-6](https://doi.org/10.1016/S1003-6326(19)64997-6).
- [39] H. DU, J. hong CAI, Y. song WANG, J. qing YAO, Q. CHEN, Y. CUI, X. wang LIU, Effect of partial recrystallization on microstructure and tensile properties of NiFeCoCrMn high-entropy alloy, *Transactions of Nonferrous Metals Society of China (English Edition)* 32 (2022) 947–956. [https://doi.org/10.1016/S1003-6326\(22\)65841-2](https://doi.org/10.1016/S1003-6326(22)65841-2).
- [40] L. Hai, J. Wang, Experimental study on the heat treatment reaction process of bentonite, *Sci Rep* 14 (2024). <https://doi.org/10.1038/s41598-024-67555-z>.
- [41] D. Chen, A. Groenvold, H.P. Rebo, K. Moljord, A. Holmen, P. Albers, S. Bösing, H. Lansink-Rotgerink, D.K. Ross, S.F. Parker, K.S. W Sing, D.H. Everett, R.A. W Haul, L. Moscou, R.A. Pierotti, J. Rouquerol, *Reporting Physisorption Data for Gas/Solid Systems*, Elsevier, 1988.
- [42] T.H. Liou, C.C. Yang, Synthesis and surface characteristics of nanosilica produced from alkali-extracted rice husk ash, *Materials Science and Engineering: B* 176 (2011) 521–529. <https://doi.org/10.1016/j.mseb.2011.01.007>.
- [43] S. Arunmetha, A. Karthik, S.R. Srither, M. Vinoth, R. Suriyaprabha, P. Manivasakan, V. Rajendran, Size-dependent physicochemical properties of mesoporous nanosilica produced from natural quartz sand using three different methods, *RSC Adv* 5 (2015) 47390–47397. <https://doi.org/10.1039/c5ra07074k>.
- [44] L.J. Cardenas-Flechas, A.M. Raba, J. Barba-Ortega, L.C. Moreno, M.R. Joya, Effect of Calcination Temperature on the Behavior of the Agglomerated Co₃O₄ Nanoparticles Obtained Through the Sol–Gel Method, *J Inorg Organomet Polym Mater* 31 (2021) 121–128. <https://doi.org/10.1007/s10904-020-01685-5>.